A

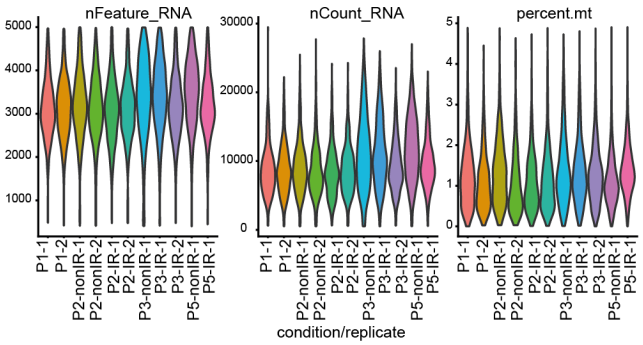

B

	P1	P2		P3		P5	
	NON-IR	NON-IR	IR	NON-IR	IR	NON-IR	IR
Replicate 1	598	564	1085	1293	896	866	2407
Replicate 2	643	826	880	-	1330	-	-
Total	1241	1390	1965	1293	2226	866	2407

C

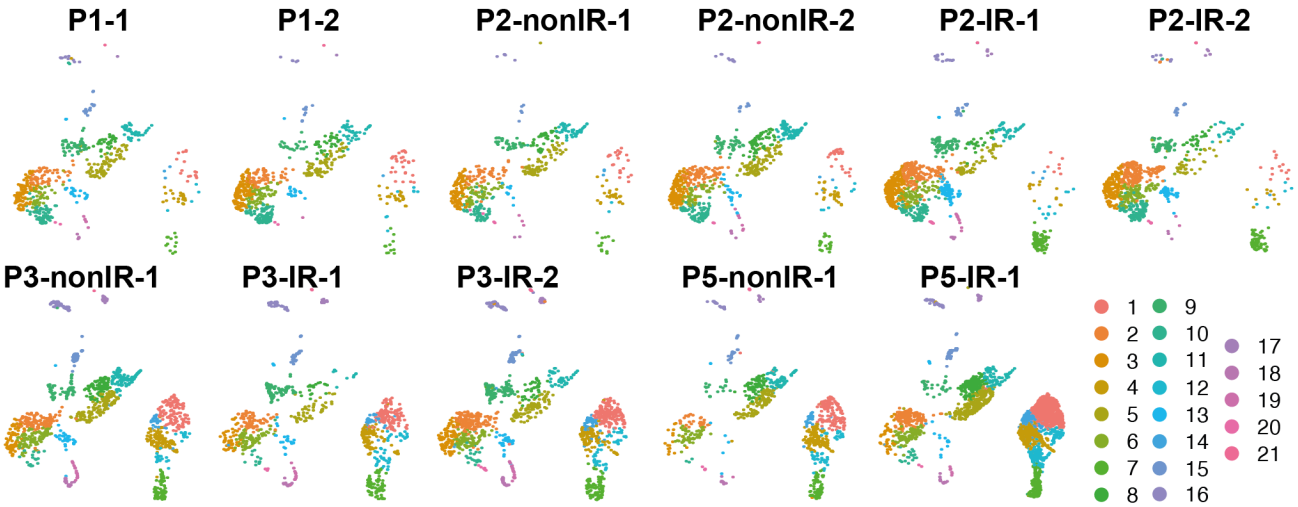

Supplementary Figure 1. scRNA-seq quality metrics and number of cells sequenced in each condition and biological replicate.

(A) Violin plots showing the number of features, RNA and percent mitochondrial RNA count across the biological replicates of the scRNA-seq data set after filtering the bad quality cells (cells were filtered out where number of detected genes was ≤ 1500, the number of detected transcripts was ≥ 40,000 and mitochondrial gene percentage ≥ 5%).

(B) Number of cells from each replicate and condition used for downstream analyses after filtering.

(C) UMAPs showing the distribution of cells across different clusters based on the samples.

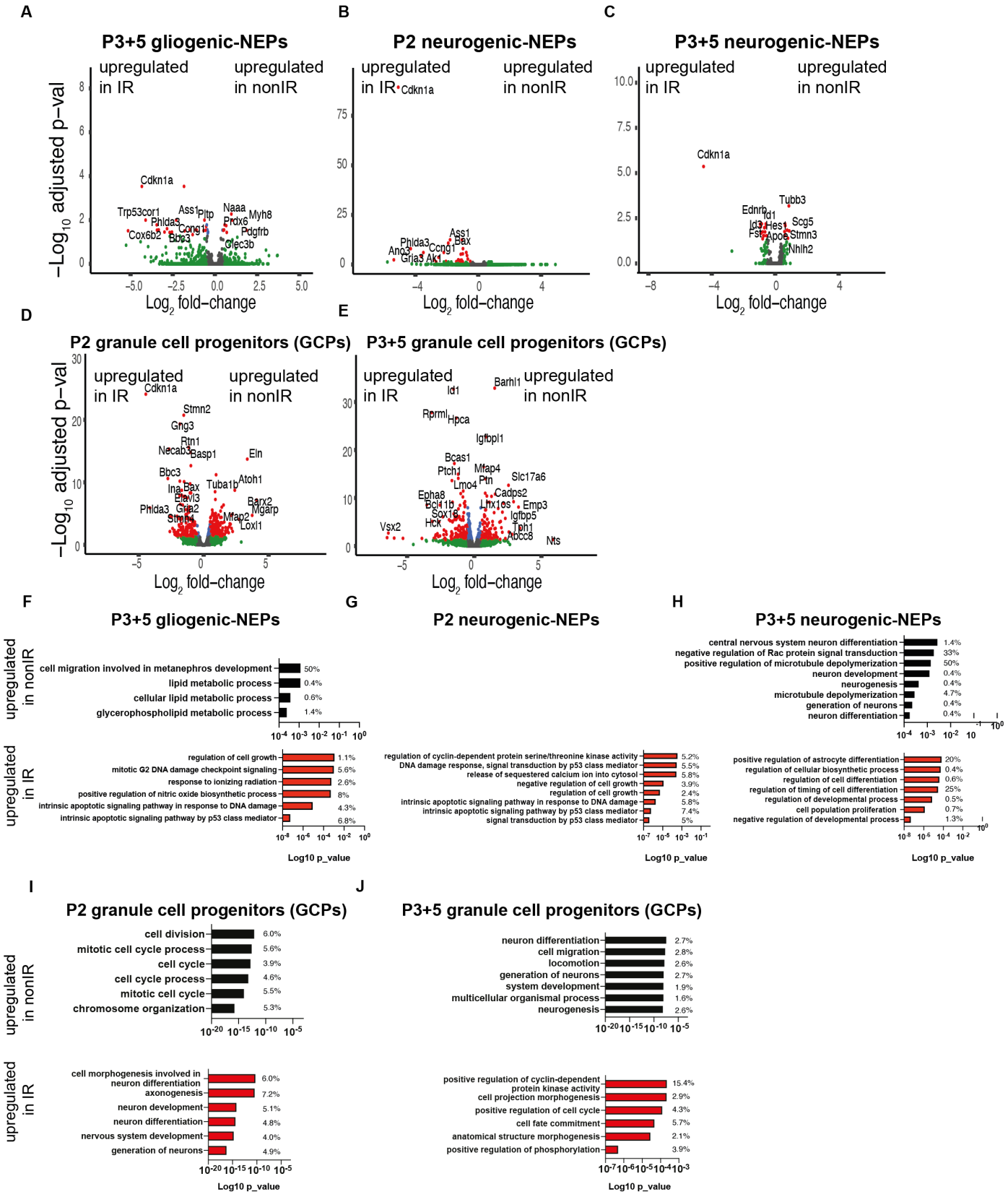

Supplementary Figure 2: Injury induces distinct transcriptional changes in NEP subtypes and GCPs during adaptive reprograming.

(A-E) Volcano plot showing differentially expressed genes in the P3+5 gliogenic-NEPs (A), P2 and P3+5 neurogenic NEPs (B, C) and P2 or P3+5 GCPs (D, E) (red: adjusted p-value≤0.05, $\log_2$fold-change=1, Table S2).

(F-J) Top GO terms associated with differentially expressed genes in the P3+5 gliogenic-NEPs (F), P2 or P3+5 neurogenic NEPs (G, H) and P2 or P3+5 GCPs (I, J) that were either upregulated in nonIR (top panel) or IR (bottom panel) (p-value≤0.05).

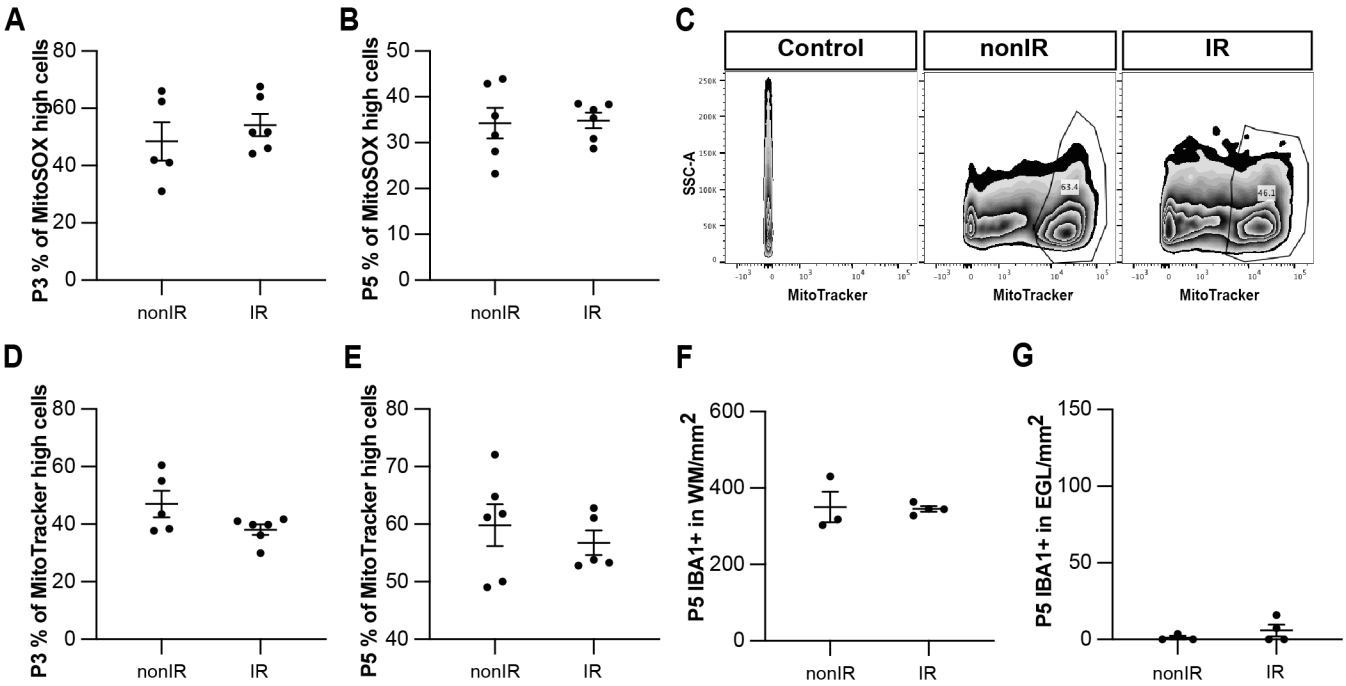

Supplementary Figure 3: Irradiation of cerebella at P1 results in increased superoxide production and cell death and recruitment of microglia to the EGL that peaks at 24h.

(A, B) Quantification of high MitoSOX expression in nonIR and IR cerebella at P3 (A) and P5 (B).

(C) Examples of flow cytometry analysis of mitochondria at P2 from nonIR and IR cerebella using MitoTracker dye. Gating determined the top 90% MitoTracker signal (MitoTracker high cells).

(D, E) Quantification of MitoTracker high expression in nonIR and IR cerebella at P3 (D) and P5 (E).

(F) Quantification of IBA1+ cell density in the WM at P5 in lobules 3-5 of nonIR and IR mice.

(G) Quantification of IBA1+ cell density in the EGL at P5 in lobules 3-5 of nonIR and IR mice.

EGL, External granular layer; WM, White matter; P, postnatal day; nonIR, non-irradiated; IR, irradiated. All statistical significance was determined using an unpaired t-test and data are represented as mean ± SEM.

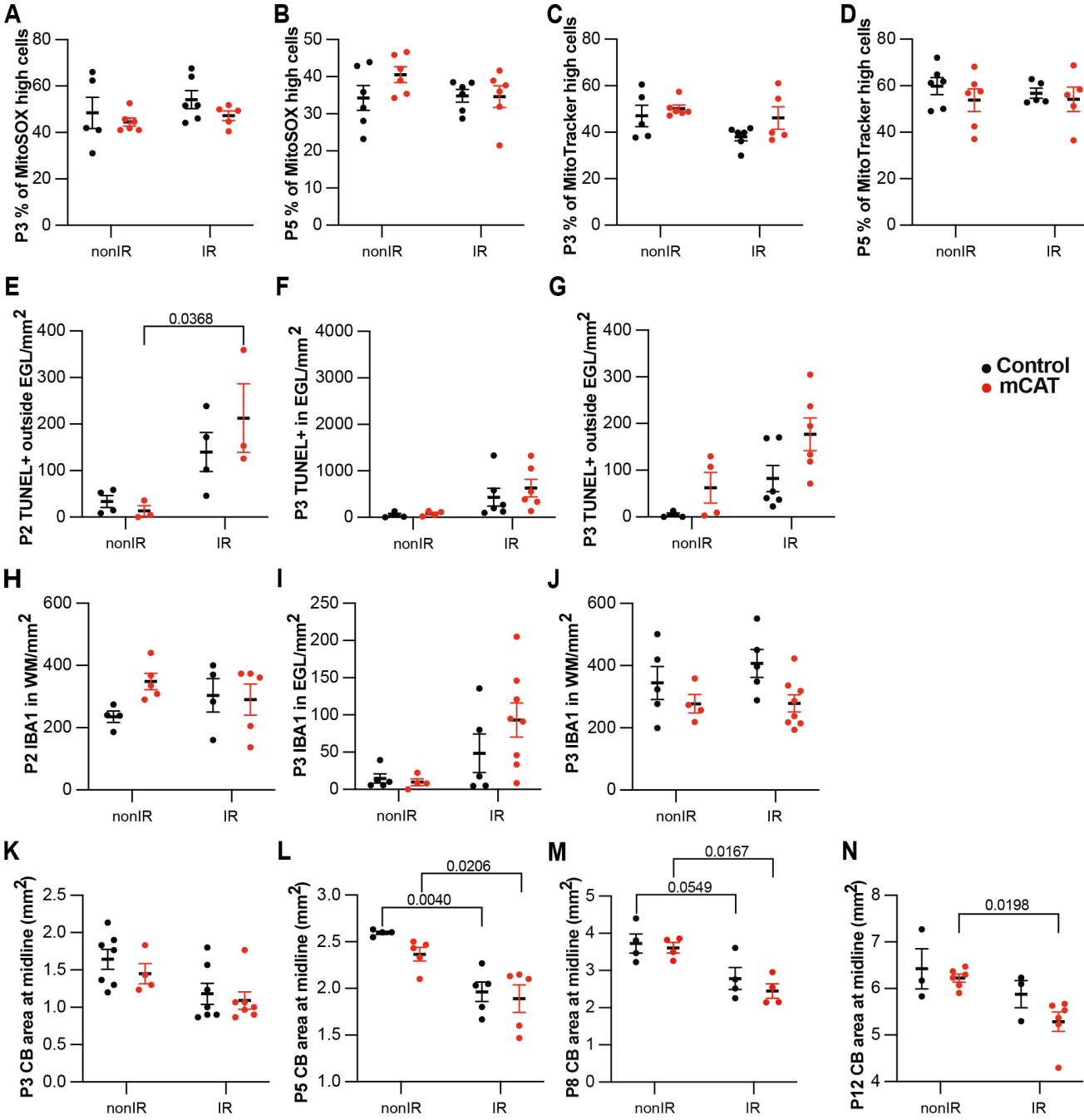

Supplementary Figure 4: Reduction of ROS impairs adaptive reprogramming and cerebellar repair.
(A, B) Quantification of high MitoSOX expression at P3 (A) and P5 (B) in control and *mCAT/+* cerebella, with and without irradiation at P1.
(C, D) Quantification of MitoTracker high expression at P3 (C) and P5 (D) in control and *mCAT/+* cerebella, with and without irradiation at P1.
(E-G) Quantification of TUNEL+ cell density outside EGL at P2 (Two-way ANOVA, $F_{(1,10)}$=14.20, p=0.0037) (E), at P3 (G), and in the EGL at P3 (F) in lobules 3-5 of nonIR and IR mice.
(H-J) Quantification of IBA1+ cell density in WM at P2 (H), at P3 (J), and in the EGL at P3 (I) in lobules 3-5 of nonIR and IR mice.
(**K-N**) Quantification of cerebellar midsagittal section area in controls and *mCAT/+* nonIR and IR mice at P3 (K), P5 (Two-way ANOVA, $F_{(1,15)}$=28.52, p<0.001) (L), P8 (Two-way ANOVA, $F_{(1,12)}$=21.21, p=0.0006) (M) and P12 (Two-way ANOVA, $F_{(1,14)}$=9.682, p=0.0077) (N).
EGL, External granular layer; WM, White matter; P, postnatal day; nonIR, non-irradiated; IR, irradiated. Significant *Tukey's post hoc* multiple comparison tests are shown in the figures and data are represented as mean ± SEM.

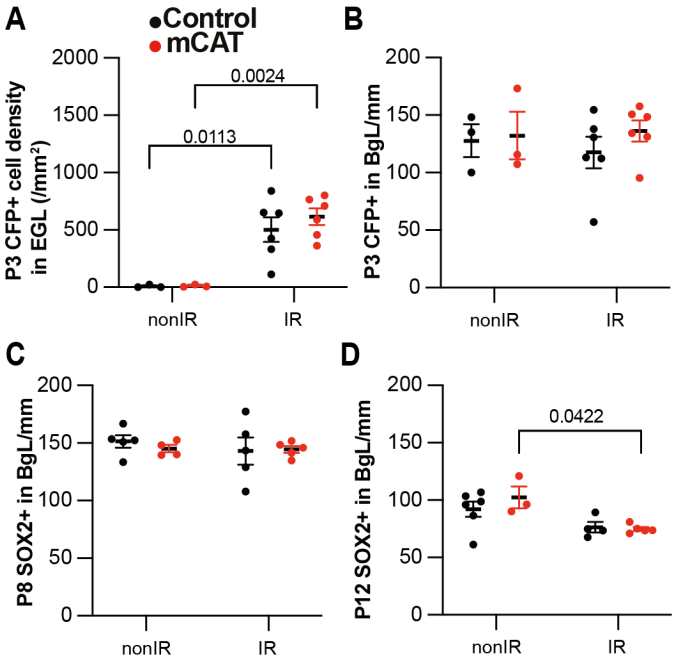

Supplementary Figure 5: Reduced ROS impairs expansion of BgL-NEPs and their migration to the EGL after injury.

(A) Quantification of CFP+ cell density in the EGL at P3 in *Nes-Cfp/+* control or *Nes-Cfp/+ mCAT* mutant nonIR and IR mice. (Two-way ANOVA, $F_{(1,14)}=33.77$, $p<0.0001$).

(B) Quantification of CFP+ cell normalized on BgL length at P5 in *Nes-Cfp/+* control or *Nes-Cfp/+ mCAT* mutant nonIR and IR mice.

(C, D) Quantification of SOX2+ NEP cell density on BgL length at P8 (C) and P12 (Two-way ANOVA, $F_{(1,12)}=12.50$, $p=0.0033$) (D) in control or *mCAT* mutant nonIR and IR mice.

EGL, External granular layer; BgL, Bergmann glia Layer; P, postnatal day; nonIR, non-irradiated; IR, irradiated. Significant *Tukey's post hoc* multiple comparison tests are shown in the figures and data are represented as mean ± SEM.

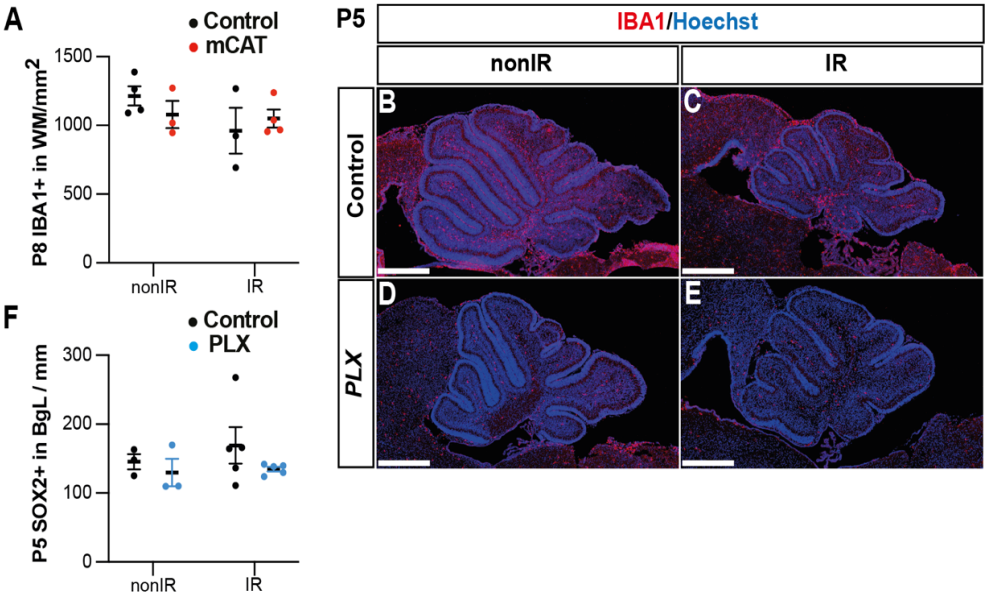

Supplementary Figure 6: Microglia promote recruitment of NEPs to the EGL during cerebellar adaptive reprogramming after injury.

(A) Quantification of IBA1+ cell density in the WM at P8 in control or *mCAT* mutant nonIR and IR mice.

(B-E) Immunostaining of medial sagittal cerebellar sections at P5 showing expression of IBA1 (red) in mice treated with PLX5622 or control DMSO, with or without irradiation.

(F) Quantification of SOX2+ NEP cell density in the BgL at P5 in control or PLX treated nonIR and IR mice.

BgL, Bergmann glia Layer; WM, White Matter; P, postnatal day; nonIR, non-irradiated; IR, irradiated. Scale bar: 500 µm. Data are represented as mean ± SEM.

Supplementary Tables

Antigen	Species	Concentration	References	Source
Catalase	Rabbit	1 to 100	01-05-030000	Athens Research & Technology
GFAP	Chicken	1 to 500	ab4674	Abcam
GFP	Rat	1 to 1000	440484	Nacalai Tesque
IBA1	Rabbit	1 to 500	019-19741	Wako Chemicals
SOX2	Goat	1 to 500	AF2018	R&D System

Table S1: List of antibodies and related information.

Table S2. Marker genes expressed by cluster in scRNA-seq dataset (irradiated at P1 (IR; P2, P3, P5) or non-irradiated (nonIR; P1, P2, P3, P5). pct1: % cells in a cluster that express the gene; pct2: % cells that express the gene outside the given cluster.

Table S3. Pseudobulk differential expression analysis between nonIR and IR gliogenic-NEPs (*Hopx+,* clusters 2, 3, 6, 10), neurogenic-NEPs (*Ascl1+,* clusters 5, 8, 11) and GCPs (*Atoh1+,* clusters 1,4,7,12,14) at P2, or at P3 and P5 (P3+5).

Table S4. GO Term analyses of differentially expressed genes (Table S3) of nonIR and IR gliogenic-NEPs (*Hopx+,* clusters 2, 3, 6, 10), neurogenic-NEPs (*Ascl1+,* clusters 5, 8, 11) and GCPs (*Atoh1+,* clusters 1,4,7,12,14) at P2, or at P3 and P5 (P3+5).

Table S5. Differentially open peaks at P2 identified by bulk ATAC-seq from nonIR and IR NEPs.

Table S6. Motif analysis of regions with increased accessibility in IR NEPs compared to the nonIR at P2.